FLEXURAL TESTING OF COLD FORMED STEEL TOP PLATE

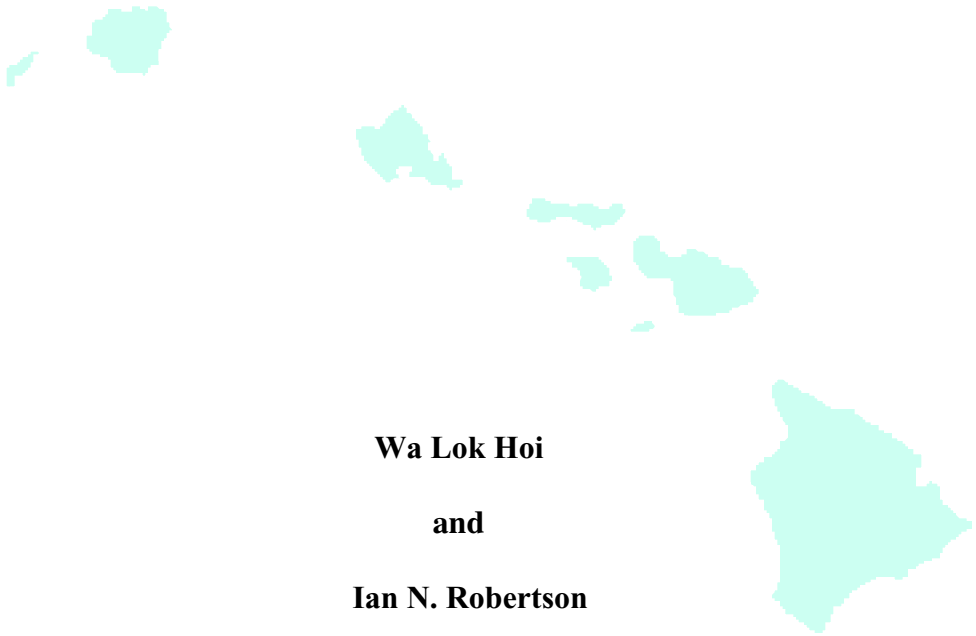

Wa Lok Hoi

and

Ian N. Robertson

UNIVERSITY OF HAWAII
COLLEGE OF ENGINEERING

DEPARTMENT OF CIVIL AND ENVIRONMENTAL ENGINEERING

Research Report UHM/CEE/05-03

December 2005

ABSTRACT

This report presents the results of a series of flexural tests performed on cold-formed steel top plates. Each top plate is a composite section created using a stud section and two track sections. Parameters considered in this study include material thickness (43-mil and 54-mil) and top plate span length (16 and 24 inch). Material tests were performed to determine the material tensile strength. Details of the testing program and its objectives are presented. A computer model was generated for each specimen to determine the AISI code allowable design load for each top plate configuration. The experimental results were compared with these analytical predictions. The AISI allowable load is approximately 30% of the proportional limit and only 22% or the experimental ultimate strength. The results are discussed and recommendations are made for design of the composite top plate section.

ACKNOWLEDGEMENTS

This report is based on a Master's Thesis prepared by Wa Lok Hoi under the direction of Ian Robertson. The authors wish to thank Drs. Gregor Fischer and Si-Hwan Park for their review of this report and their suggestions for improvement. The authors are grateful to Gaur Johnson for his assistance in instrumentation of the test specimens during the experimental program.

This project was initiated by members of the Hawaii Light Gauge Steel Engineers Association (LGSEA) research committee. Cold-formed steel research at the University of Hawaii enjoys continued support from the Hawaii Chapter of LGSEA and the Hawaii Pacific Steel Framing Alliance (HPSFA), which is greatly appreciated. All materials used in fabricating the test specimens were donated by Dietrich Metal Framing. Akira Usami is thanked for facilitating this contribution, which is gratefully acknowledged.

TABLE OF CONTENTS

TABLE OF FIGURES

TABLE OF TABLES

1 Introduction

1.1 Background

Home construction in the USA has historically been a wood-frame based industry. However, cold-formed steel (CFS) has made numerous inroads into residential construction, particularly in Hawaii. CFS possesses a set of material properties that qualify it as a good structural material. CFS sections used in residential construction are lightweight, non-flammable, insect-resistant, and can be manufactured to virtually any shape and dimension with limited loss of material. Steel is also dimensionally stable since it is not subject to shrinkage, twisting or warping. With adequate galvanizing and other protective measures, CFS can be protected from corrosion, the only major environmental decay mechanism affecting steel.

From an economical standpoint, the future uncertainty of global wood supply implies that the cost for lumber will increase. When a traditional home is demolished, the building material is usually wasted. However, in steel construction, the material can be reprocessed into new building material.

Current residential construction using steel framing is very similar to traditional wood framing. CFS structural members have been produced with similar dimensions to traditional wood members to simplify transition from one material to the other. One notable difference between CFS and wood construction is the need for concentric framing in CFS construction due to the lack of a strong top plate at the top of load-bearing stud walls. Joists or rafters supported on a stud wall must be aligned with the supporting studs because the simple track section at the top of the wall is not adequate to distribute non-concentric loads. In timber construction, the double “2 by 4” top plate serves this function.

This poses a challenge to both builder and designer. For example, a designer who wants to space the floor joists or roof rafters at different spacing than the wall studs would be limited to the smaller spacing or spend extra resources to develop an engineered load distribution member. Both of these options will increase the cost of the structure. Field alterations to floor and roof framing are also limited by the need to align with the framing members below.

This report presents the details and results of an experimental study conducted in the Materials Testing Laboratory of the University of Hawai‘i for the Light Gauge Steel Engineers Association (LGSEA) in an effort to develop a feasible top plate configuration for CFS framing.

1.2 Objective of Project

The specific objectives of this project are as follows:

1. To investigate the load-deflection response of a composite top track under static loading conditions.
2. To investigate the ultimate and service capacity of each configuration based on the test results.
3. To compare the design strength from an Allowable Stress Design LGBeamer computer analysis with the experimental results.
4. To develop design guidance for use of the composite top track system in CFS construction.

1.3 Scope

This study began with a review of recent or current research related to topics about load bearing top plates. The current code for cold-formed steel was also reviewed.

The experimental component of this study involved fabrication and load testing of 12 CFS top plate specimens. The specimens were separated into four-groups based on their gauge thickness and span length. All specimens used a composite top plate section, which consists of two tracks and a stud. Both 54-mil (16-gauge) and 43-mil (18-gauge) track and stud sections were used. Based on typical wall stud spacing, 16 and 24 inch spans were selected for the test specimens. All tests were performed using a servo-controlled hydraulic test frame. Deflections were measured using Linear Variable Differential Transducers (LVDTs) located at midspan in each span.

An analytical study was performed based on the "American Iron and Steel Institute (AISI) "Specification for the Design of Cold-Formed Structural Members" 1996 edition with 1999 supplement. The results were then compared with the experimental results.

1.4 Outline

Chapter 2 of this report summarizes two recent studies of various load bearing top plates. In chapter 3, a brief description of previous work conducted in the Materials Testing Laboratory of the University of Hawai‘i is given. The current experimental program is described in chapter 4. All results from this study are presented in chapter 5. Chapter 6 introduces the computer model used to determine analytical capacity and its results. Comparisons between the analytical and experimental results are presented in chapter 7. Finally, chapter 8 contains a summary and conclusions to the report.

2 Literature Review

2.1 Overview

Very little research has been performed in the area of load-bearing cold-formed steel top plates. This chapter summarizes two recent independent studies. The two studies were conducted by the National Association of Home Builders (NAHB) Research Center, and the Structural Engineering Laboratory of the University of New Brunswick.

2.2 NAHB Report

In August 2002, the NAHB Research Center conducted a series of tests to investigate the feasibility of three different configurations of steel load-bearing top plate (NAHB 2002). At the time of the study, little research was available on this topic. The report noted that Australian researchers had developed several shapes for load distribution members.

The main objective of the study was to evaluate three different configurations for the top plates. The three configurations were as follows: a deep leg track, a wood top plate (2 x 4 wood plate nailed to a standard track) and a J-track. All specimens were two-span with 24 inch stud spacing while loads were applied at the midspan of each span. Twenty-one specimens of various material thicknesses were tested in the study. Based on the LRFD design provisions of the AISI specification, a resistance factor was computed and design aids developed.

The behavior of the three configurations were as follows:

1. All deep leg track specimens started to show signs of local buckling at the load bearing point at approximately 65 percent of the ultimate load, and the specimens ultimately failed in localized buckling at the load points.

2. All specimens with 2x4 top plates ultimately failed in bending, but the top track did not show any signs of local buckling, and track sections were not severely deformed at the ultimate load.

3. J-track specimens failed in localized buckling at the load points. However, the nonsymmetrical shape of the J-track created concentrated loading at the stiffer side of the track and lowered the load sharing between flanges.

The report concluded that all three configurations could be used as load distribution members for light-frame cold-formed steel structures with 24-inch maximum stud spacing. It was determined that the strongest configuration was the combination of 33 mil (0.033inch) (20-gauge) top track and 2x4 wood top plate.

2.3 University of New Brunswick Report

The Structural Engineering Laboratory of the University of New Brunswick published the results of their study in September 2005 (Dawe 2005). Five groups of specimens were tested in the study, constituting 60 specimens in all. Each group consisted of a 54-mil (16-gauge) or 43-mil (18-gauge) track supported on studs at 16 and 24 inch spacing. A theoretical analysis was also completed for comparison.

The specific objective of the study was to determine the experimental value of strength and stiffness for the following top plate configurations:

1. Standard top track and 2x4 wood top plate on 3-5/8 inch stud wall
2. Standard top track on 3-5/8 inch stud wall
3. Standard top track and 2x6 wood top plate on 6 inch stud wall
4. Standard top track on 6 inch stud wall

5. Deep Leg top track on 3-5/8 inch stud wall

Twenty-four inch span specimens were loaded at mid-span for each span. Sixteen inch span specimens were loaded at the mid-span of the left span and directly above the right stud support. The loading rate was constant at 1kN/min until ultimate capacity was reached.

Buckling of the legs of the top track was a common failure mechanism for all specimens. The results indicated that all specimens benefited from the addition of a wood top plate. In general, the gain in the capacity largely depended on the capacity of the wood top plate. The 24-inch spaced and 18-gauge specimens benefited the most from the wood plate. The ultimate load was increased significantly. In comparison, shorter spans and thicker steel had a less significant increase in capacity.

The following conclusions were drawn as a result of this research:

1. Specimens with heavier gauge steel tracks developed higher capacities than lighter gauge steel tracks.
2. For specimens of the same gauge, shorter spans had higher ultimate loads with lower deflections.
3. Specimens with a wood top plate were significantly stronger and had less deflection than those without. Weaker specimens benefited the most from the addition of the wood top plate.
4. The deep leg track resisted a higher load than the standard tracks. Deformation occurred locally at the load point rather than over the supports, indicating a higher resistance to flexure than to local crippling.

3 Previous UH Studies

3.1 Introduction

A number of prior test series on cold-formed steel top plates have been performed in the Material Testing Laboratory at the University of Hawaii. These tests were performed as group projects as part of both graduate and undergraduate courses on structural steel design during 2003 and 2004.

3.2 Initial Test Specimens

The initial test specimens were fabricated by industry collaborators, and consisted of three spans supported by four studs. Sections of roof trusses were connected to the top plate by means of hurricane clips at midspan of the outer two spans. These specimens were tested as a class project in the undergraduate course, CEE 486 – Structural Steel Design. Because of the complexity of these specimens, the results could only be applied to identical configurations, but could not be extended to general field conditions. The results therefore did not have general benefit for different framing configurations. These results are not used in the present study.

3.3 Phase I Test Specimens

A series of tests was performed by graduate students in CEE 685 – Advanced Structural Steel Design. This series consisted of specimens with two spans supported on three studs, similar to those tested in the current study. The top plate sections were fabricated from 33-mil, 43-mil and 54-mil plate; however the top track section was consistently 43-mil material. This resulted in a non-typical condition where the various components of the composite top plate were not all the same material thickness. In addition, it was noted that some of the load-

displacement plots varied significantly from presumably identical specimens. It was later discovered that there were errors in some of the section thicknesses.

In addition, some of the stud sections used in the composite top plate had punch-outs for electrical conduits, while others did not. This resulted in almost 10% variation in ultimate load capacity.

In order to investigate the benefits of improved composite action, additional screws were added to the top plate to try and force the two tracks and one stud section to work as a fully composite section. It was determined that an uneconomically large number of screws would be required to produce truly composite action.

It was also noted that the 33-mil top plate sections tended to fail due to lateral buckling of the box-section created by the stud and track in the top plate. This was considered an undesirable failure mode and so no further tests were performed with 33-mil top plate sections. Because of inconsistency in section thickness, and presence of punch-outs, the results of this phase of testing are not included in the current study.

3.4 Phase II Test Specimens

A second phase of tests was performed as a class project in CEE 486 – Structural Steel Design. This series of tests were similar to those in Phase I above, but consisted of some specimens without punch-outs in the stud section, some with punch-outs at the center support, and others with punch-outs at midspan of the top track spans. The results confirmed that the punch-outs do reduce the ultimate strength of the composite top plate by approximately 10%; however the location of the punch-out had no significant effect on this reduction in strength. The results of this testing were not used in the current study.

3.5 Lessons applied to the current study

Based on the phase II testing described above, all stud sections used as part of the top plate included punch-outs located over the center support. This configuration was selected as it represented the weaker condition of sections with or without punch-outs, and under field conditions, it may not be possible to ensure that stud sections used in the top plate have no punch-outs. No top plate sections were fabricated using 33-mil material thickness because of the undesirable lateral buckling failure mechanism observed in the prior studies. A minimum number of screw fasteners was used to construct the composite top plate element.

4 Experimental Program

4.1 Introduction

A top plate that provides adequate strength and stiffness is highly desirable in the design of economical steel framing systems. The main objective of this study is to investigate the behavior at both service and ultimate capacity of a composite top plate. Four groups of tests were conducted using twelve track and stud specimens of 43-mil and 54-mil thickness, spanning either 16 or 24 inches. Material testing was also conducted on test coupons cut from the studs and tracks.

4.2 Fabrication

4.2.1 Specimen Designation

Specimens are designated according to their thickness in mil (0.001in) and their center-to-center stud spacing. For example, specimen designation T16-43C1 indicates a top plate supported on studs with a 16 inch center-to-center spacing, using 43-mil tracks and stud in the composite top plate section. C1 is the designation for specimen number 1 in the group.

4.2.2 Top Plate Composite Section

All specimens have identical top plate configuration. The top plate section consists of one 350S162 stud and two 350T150 tracks. Details of the stud and track sections are shown in Figure 4-1. The section thickness (t) was either 43-mils or 54-mils. Figure 4-2 shows a schematic of the composite top plate, while Figure 4-3 shows a typical top plate on a test specimen.

A stud and two track sections were used to form the composite top plate section. Number 10 self-drilling and taping screws were used for all connections. The stud and one track section were nested to form a box section. Three screws were used on each side (one above each

support stud) to secure the box section. A track section was then connected to the stud to form a back-to-back connection using six more screws. This track section was then connected to the top of the supporting studs with one screw in each flange. For a particular composite top plate, both tracks and stud had the same thickness.

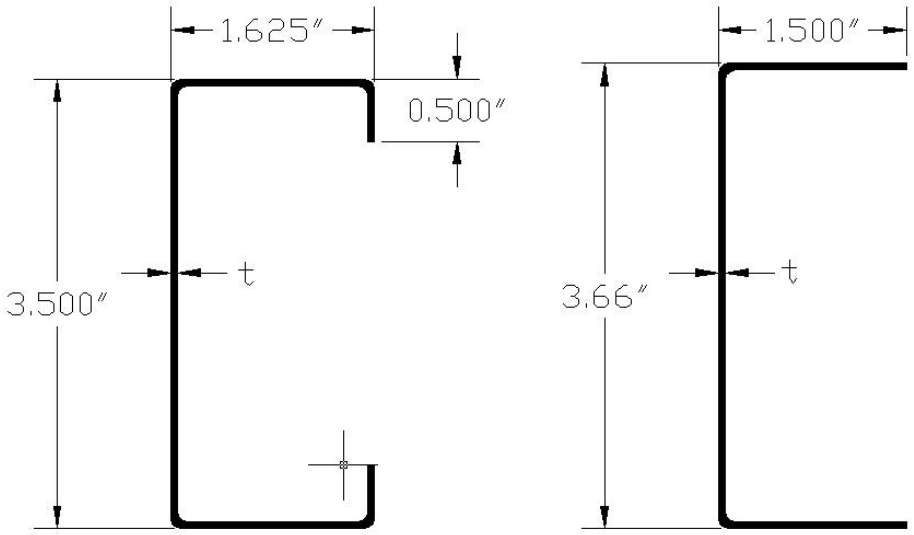

Figure 4-1: Stud and Track Section Details.

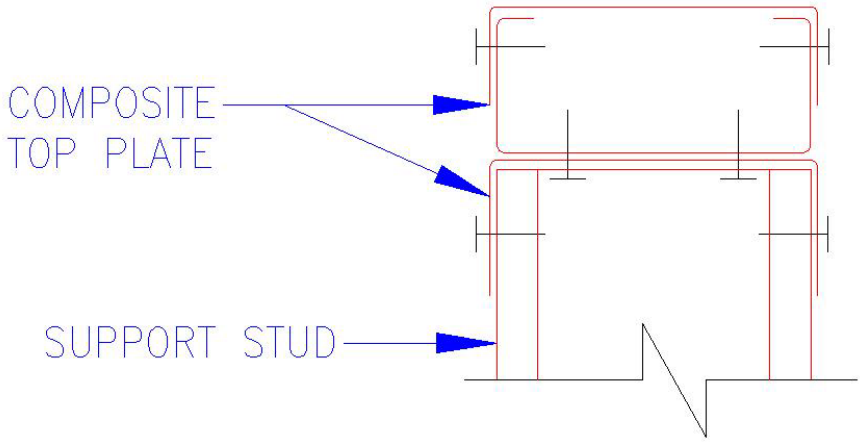

Figure 4-2: Typical Top Plate Configuration

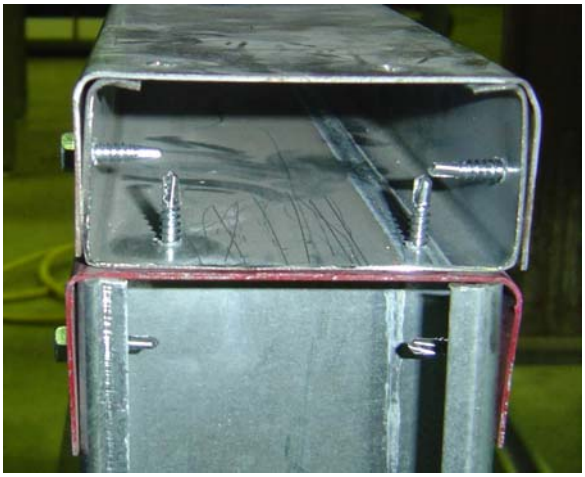

Figure 4-3: Typical composite top plate section

4.2.3 Specimen Fabrication

All specimens were constructed as a frame as shown in Figure 4-4. Three 18" tall stud sections spaced at 16 or 24 inches were used as supports for the top plate. A bottom track was used to secure the bottom of each stud, while an additional track section was added to each side of the frame as a brace to prevent racking. Twelve specimens were fabricated for this study and separated into four groups according to their span length and gauge thickness. Table 4.1 lists the complete details of all specimens tested in this study.

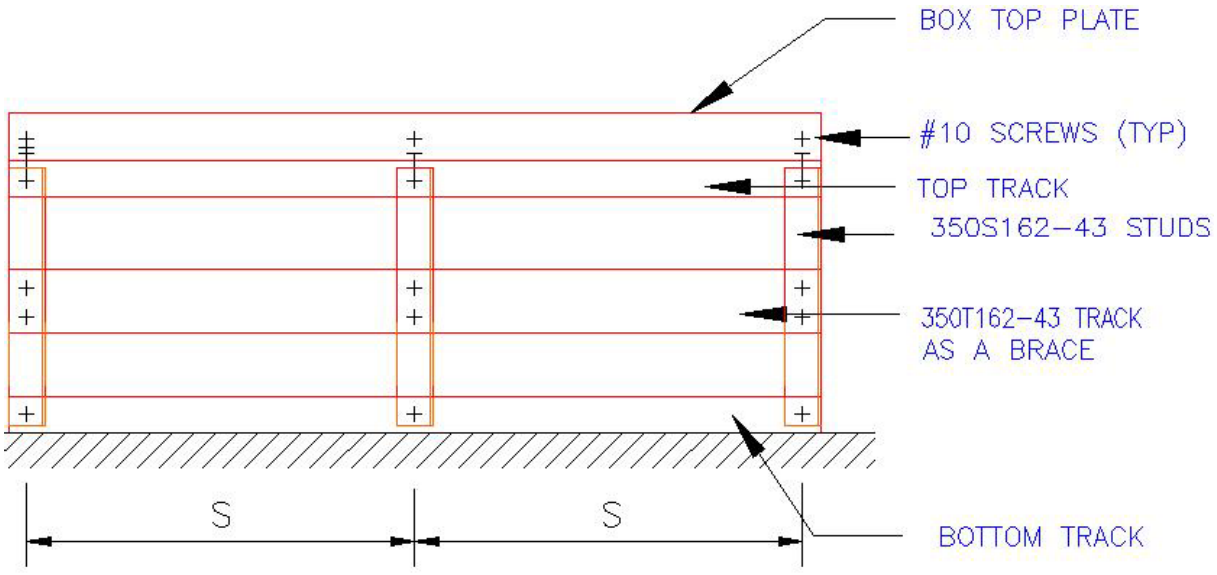

Figure 4-4: Typical Specimen Details

Table 4.1: Fabrication Details of Test Specimen

Specimen	Thickness (t) (inch)	Spacing (S) (inch)
T16-43C1---C3	0.043	16”
T24-43C1---C3	0.043	24”
T16-54C1---C3	0.054	16”
T24-54C1---C3	0.054	24”

4.2.4 Material Sample Fabrication

Three test coupons were extracted from samples of the stud and track sections for material testing. The dimensions of the test coupons were 1” wide by 18” long. In order to avoid any property changes associated with heating, all samples were cut out using an electric hand shear. These coupons were tested in direct tension in a 55,000 lb. MTS hydraulic test frame.

4.3 Test Setup

The typical setup for a top plate specimen test is shown in Figure 4-5 and Figure 4-6**.** Two equal loads were applied at mid-span of each span. An aluminum wide flange beam was used to distribute the load from the hydraulic actuator to the two loading points. A Linear Variable Differential Transducer (LVDT) was placed directly on top of the distribution beam at each loading point for displacement measurements. A separate frame was built to support the LVDTs so that movement of the hydraulic frame would not affect the deflection readings. A 1.5” wide by 4” long steel bearing plate was placed between the distribution beam and the specimen at each load point to simulate the bearing area of a joist or rafter in typical construction. The total applied load was monitored by a load cell. The load cell and LVDT measurements were recorded by a National Instruments Data Acquisition System running Labview. The data acquisition sampling rate was set to 10 readings per second. A steel plate

was placed under the specimen and low-carbon steel shim stock was used to level the specimen. No restraint was used to secure the specimen to the ground.

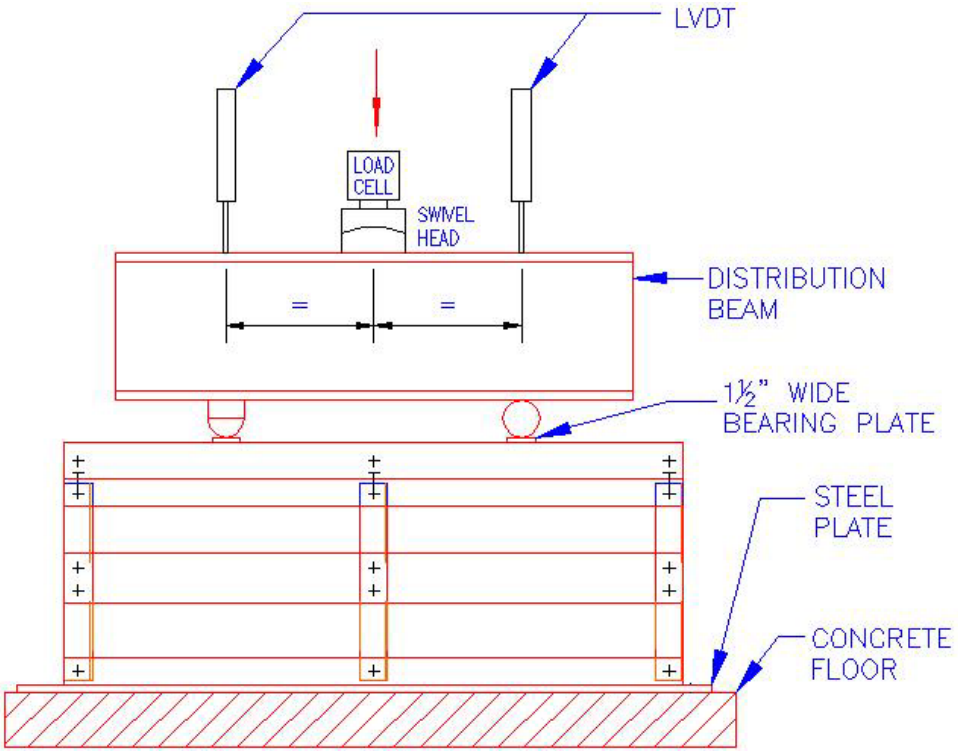

Figure 4-5: Test Setup Schematic

Figure 4-6: Typical Test Specimen in Test Frame

4.4 Testing Procedure

Specimens were placed directly below the hydraulic actuator. Leveling was performed on each specimen in order to prevent non-vertical loading. The bearing plates and distribution beam were then placed on top of the specimen. The hydraulic actuator was lowered onto the specimen with an applied force of approximately 100 pounds. It was then raised to decrease the force to less than 10 pounds. Automated loading, under displacement control, was then initiated at a constant rate of 0.005 inch/sec. Loading was paused to allow visual inspection of the specimen at the estimated yield point and at the ultimate load.

4.5 Instrumentation

4.5.1 Linear Variable Differential Transducers (LVDT)

Deflection measurements were made using two LVDTs installed on the top of the load distribution beam. The LVDT was chosen over other displacement transducers because of its high degree of accuracy and repeatability. The principle of measurement used in LVDTs is based on magnetic transfer, which does not require physical contact with the sensing element and eliminates errors caused by wear and tear of equipment, thus contributing to its repeatability. With suitable signal conditioning electronics, very small movements can be detected.

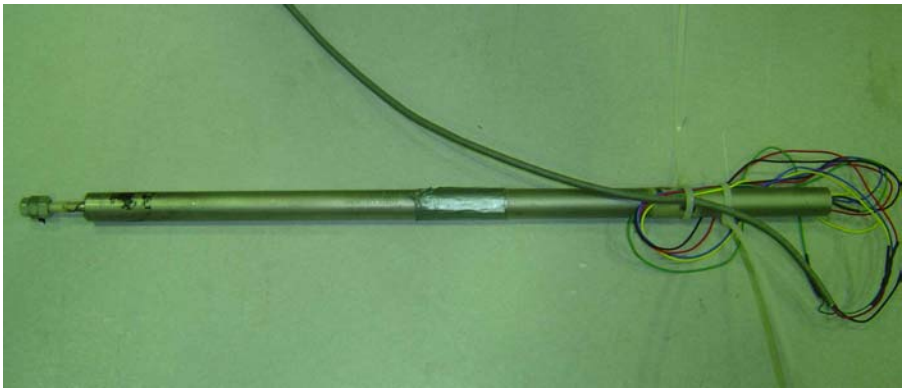

Figure 4-7: LVDT Used for Deflection Measurement

4.5.2 Hydraulic Test Frame

A 300,000 lb test frame controlled by a MTS TestStar II servo-controller was used to load the specimens (Figure 4-9). A load cell was used for load measurements, and was monitored by the data acquisition system for data recording. The MTS controller provides accurate control of movement of the hydraulic actuator at the selected loading rate (Figure 4-8).

Figure 4-8: MTS TestStar II Servo-Controller

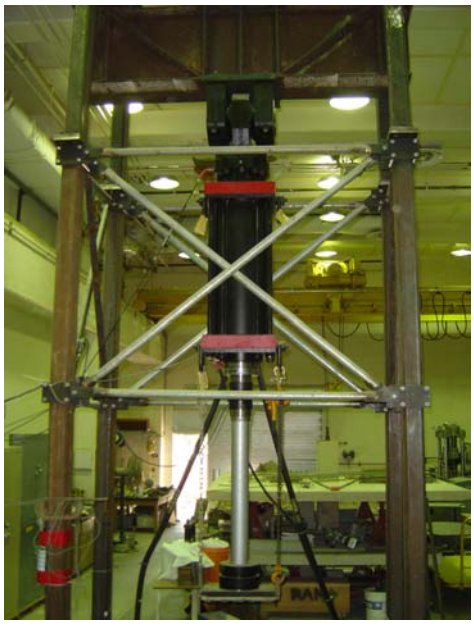

Figure 4-9: Hydraulic Test Frame

4.5.3 Data Acquisition System

For data collection, a National Instruments multi-channel data acquisition system running Labview Version 7 Express was used (Figure 4-10). Both LVDTs and the load cell were

connected to the system and data was monitored at a sampling rate of 10 readings per second simultaneously on all channels.

Figure 4-10: Data Acquisition System

4.5.4 MTS Material Testing System

A MTS 810 Universal Servo-controlled Test Frame was used to test the steel coupons as shown in Figure 4-11.

Figure 4-11: MTS 810 Material Test Frame

4.6 Data Processing

4.6.1 Specimen Data

As illustrated in Figure 4-12, typical load-displacement curves obtained from the raw data do not start from the origin because the LVDTs were not zeroed before each test. They also

show a non-linear "setting in" period at the start of loading. To allow for comparison of different specimen response, all data were zeroed. The linear elastic portion of the load-displacement data was extracted from the data series. Using the equation acquired from regression analysis, the curve was shifted by the amount of the x-intercept. The non-linear region in the beginning of the curve is discarded, and the linear region is extended to the origin. Figure 4-12 shows the resulting processed plots once the LVDT data has been zeroed and the initial non-linear response removed. These adjustments to the raw data have no effect on the measured load, and only a minor effect on the measured deflections.

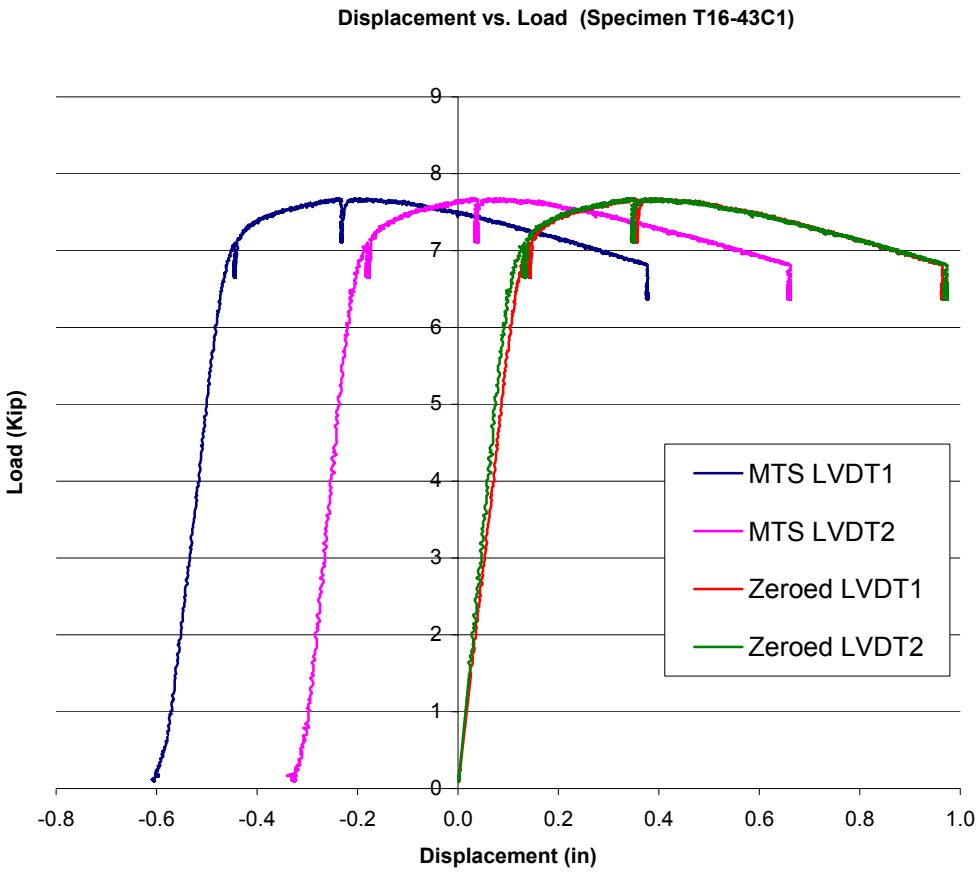

Figure 4-12: Typical Raw Data Plot

Figure 4-12 shows the typically good agreement between the two LVDTs in adjacent spans of the test specimen. These displacement measurements from the two spans were then averaged to give a single load-displacement plot for each specimen. The load reading recorded by the load cell installed on the hydraulic actuator is the total applied load. This load was divided by two for the single span load.

The average load-displacement curves for all three specimens in the same test series were then plotted together for comparison. A sample comparison for T16-43 is shown in Figure 4-13. Similar load-displacement plots for all four test series are included in Appendix B.

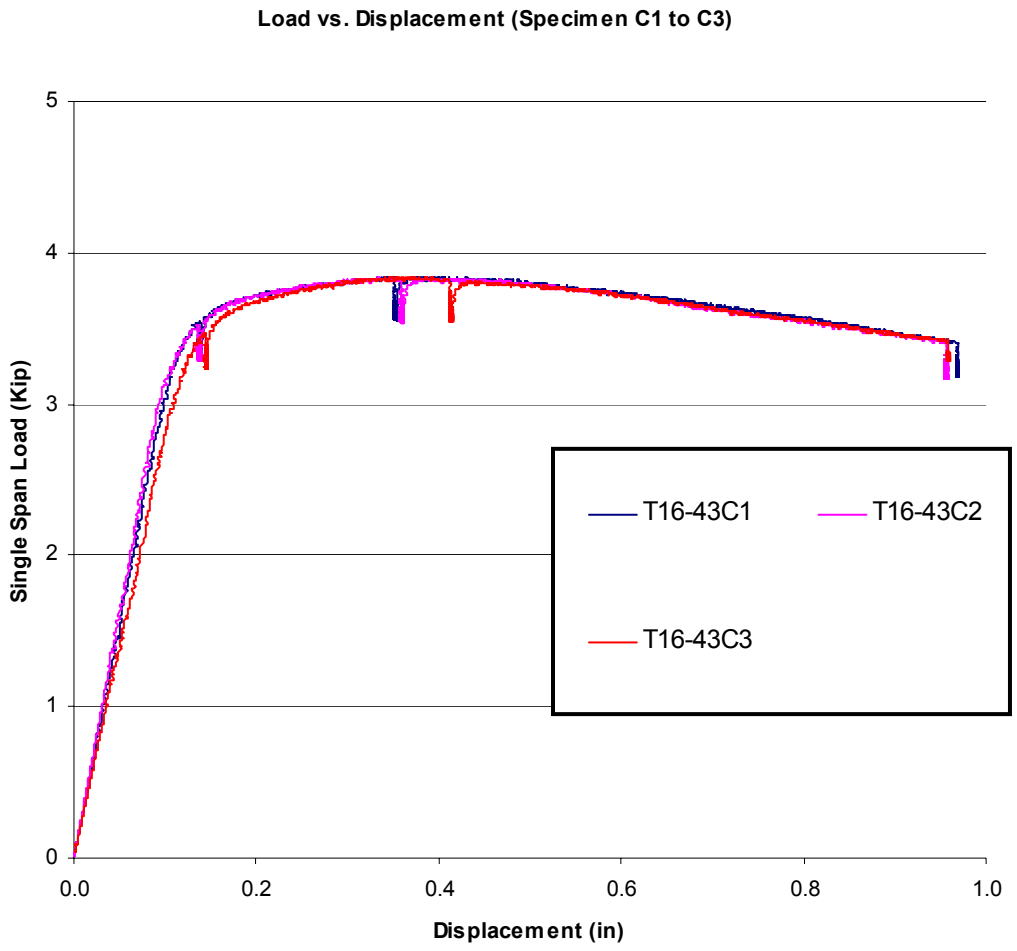

Figure 4-13: Typical Group Load-Displacement Plot

All test specimens show a smooth transition from elastic to plastic behavior with no well-defined yield point. The proportional limit represents the elastic limit of the composite section. The value for the proportional limit was acquired by extending the regression line past the linear region, and visually identifying the point of separation between the two lines as shown in Figure 4-14. Also shown in Figure 4-14 is the maximum load supported by the specimen, identified as the ultimate capacity, and the corresponding deflection.

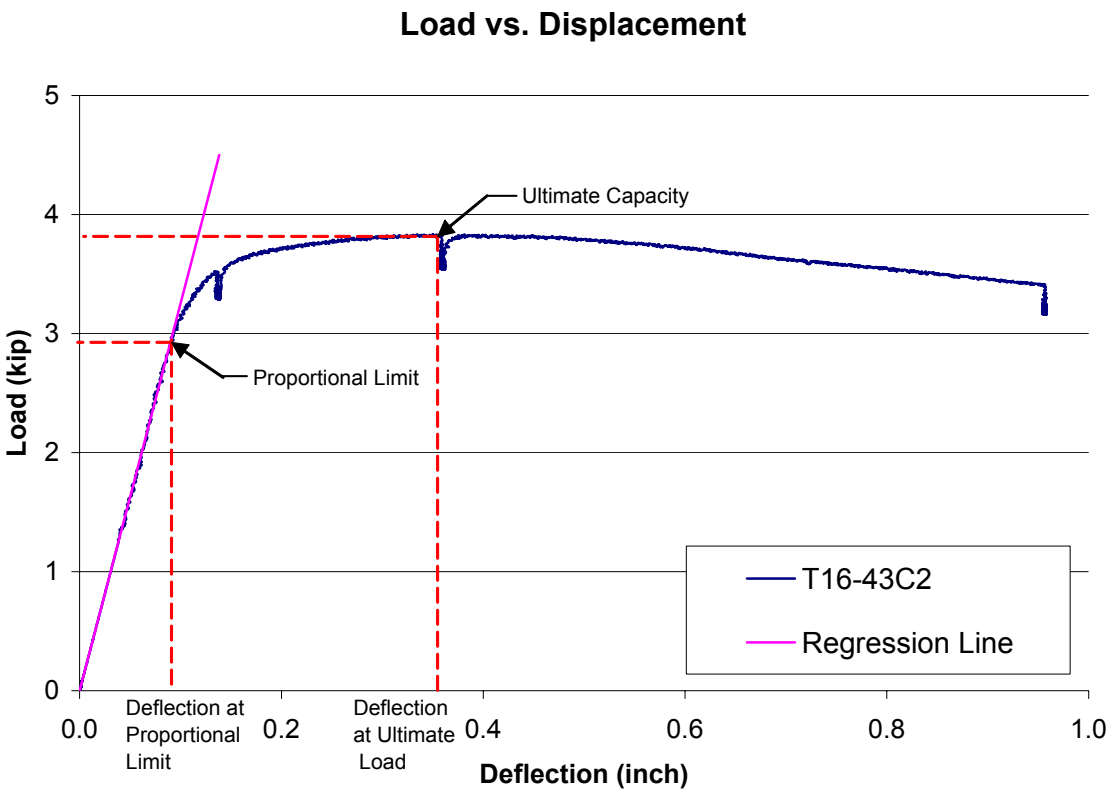

Figure 4-14: Typical Load-Displacement Plot with Regression Line and Proportional Limit

4.6.2 Material Coupon Testing and Data Processing Procedure.

Before testing, the dimensions of each coupon were measured at both ends of the coupon. Cross-sectional areas were based on the average dimensions. Each coupon was tested over a 12 inch gauge length between hydraulic grips in the MTS load frame. Stress was calculated

by dividing the load reading by the cross-sectional area. Average strain was calculated by dividing the displacement reading by the gauge length of 12 inches. Stress and strain were then plotted on a typical stress-strain curve as shown in Figure 4-15.

For samples that did not have a well defined yield point, the yield stress was determined using the 0.2% offset method as shown in Figure 4-15. The yield point was defined by the intersection of the 0.2% offset line and the stress-strain curve.

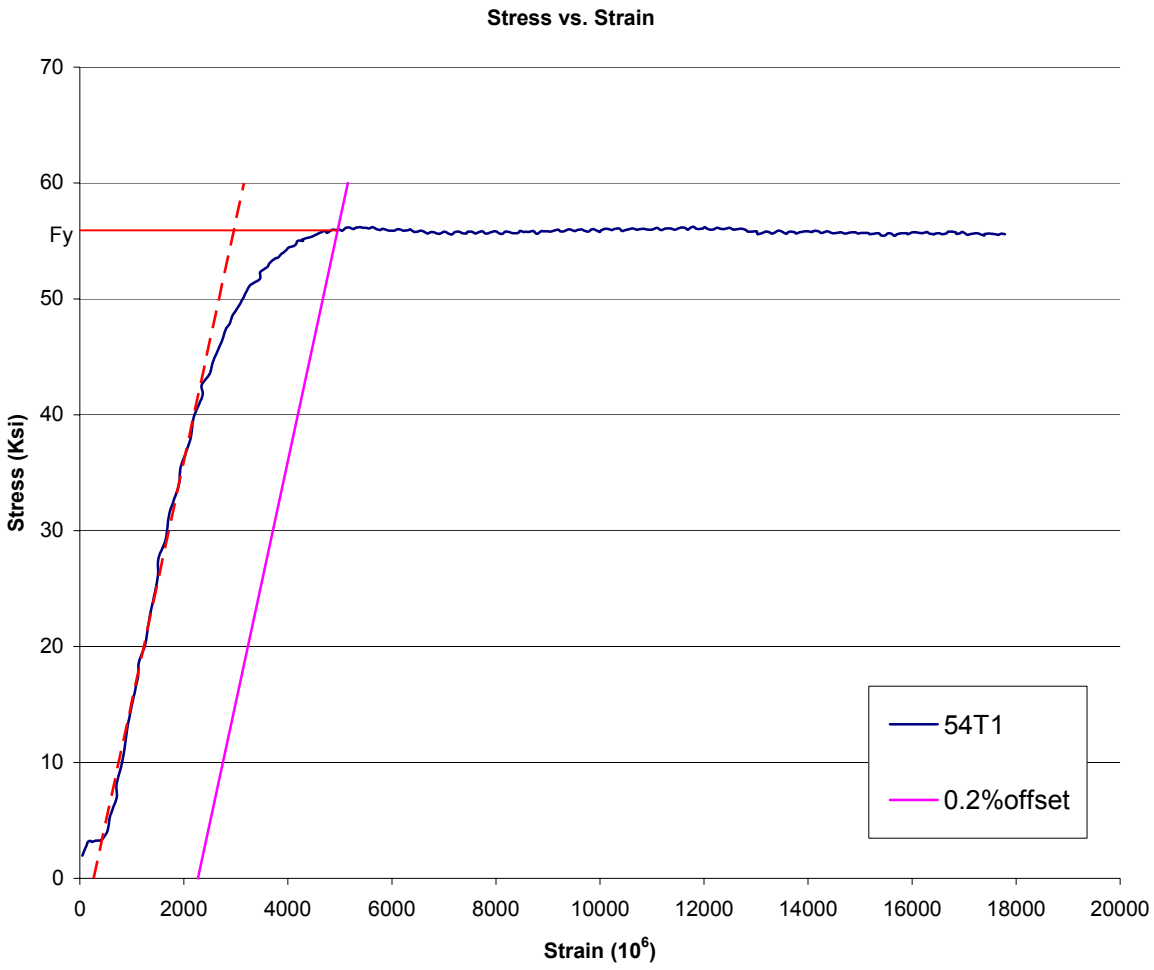

Figure 4-15: Typical Material Coupon Stress-Strain Curve with 0.2% Offset Line.

5 Test Results

5.1 Overview

Both material testing and specimen test results are presented in this chapter. All values listing ultimate loads and proportional limits are based on the load on a single span. A typical top plate test specimen response is described in this chapter, followed by presentation of all results from material testing and the top plate specimen tests.

5.2 Test Description

All specimens behaved the same in their elastic region. Very small deflections were observed before the proportional limit. Once the specimen response became non-linear, lateral buckling started to occur in the flanges of the track section at the center support (Figure 5-1). Near ultimate load, local bearing failure was noted under both loading points (Figure 5-2). All specimens ultimately failed due to flexure and local buckling resulting in a gradual reduction in load with increasing deflection after the ultimate load (Figure 5-3).

For all but one specimen, the deflections measured at mid-span of the two adjacent spans were nearly identical during the test. For specimen T24-43C1, from initial loading to yielding the deflection was similar. However, shortly after entering the inelastic region deflections in one span increased more rapidly than the other.

Premature stud failure was noted in the middle support of specimens in test group T16-54. Local buckling in the track legs may have initiated the stud failure by pushing the stud legs inward (Figure 5-4). Buckling failure of the center stud support occurred after the ultimate load had been reached (Figure 5-3). A sudden decrease of load carrying capacity associated with this buckling is evident in the load-displacement plots for these specimens (Figure 5-5).

Figure 5-1: Lateral Buckling of Track Flanges at Center Support

Figure 5-2: Specimen at Ultimate Load

Figure 5-3: Failure of Specimen

Figure 5-4: Buckling Failure of Support Stud After Flexural Failure of Top Plate

5.3 Material Yield Stress

Table 5.1 lists the individual and average yield stresses for the twelve material coupons extracted from the stud (S) and track (T) sections used in this study. As the results indicate, the yield stress is consistently higher than the nominal strength. The 43-mil coupons from both stud and track sections have significant higher yield strength than the nominal 33 ksi listed in the AISI specification. On average, the stud sections were 33% stronger while the track sections were 53% stronger than the nominal 33 ksi yield stress. The 54-mil coupons were approximately 10 percent higher than the nominal 50 ksi listed in the AISI specification.

Table 5.1: Material Sample Yield Stress

Sample	Nominal Thickness (mil)	Nominal Strength (ksi)	Average Thickness (mil)	Average Width (in)	Yield Stress (ksi)	Average Yield Stress (ksi)
43S1	43	33	45	0.994	43.99	43.88
43S2	43	33	45	1.004	43.66	
43S3	43	33	45	1.001	43.98	
43T1	43	33	44	0.997	51.49	50.59
43T2	43	33	44	1.040	51.21	
43T3	43	33	44	0.985	49.06	
54S1	54	50	55	1.095	58.04	55.88
54S2	54	50	55	1.033	54.55	
54S3	54	50	55	1.006	55.06	
54T1	54	50	54	1.000	55.90	55.22
54T2	54	50	55	0.997	54.55	
54T3	54	50	55	0.998	54.22	

5.4 Proportional Limit

Table 5.2 lists the proportional limits and their corresponding vertical deflections for all top plate test specimens. Average values are also listed, as are correlation coefficients of the linear regression analysis used to determine the proportional limit.

Table 5.2: Proportional Limit and Corresponding Deflection

Specimen	P.L. (kip) (1)	Deflection (in) (2)	C.F. (R^2)	Average P.L. (kip)	Average Deflection (in)
T16-43C1	2.800	0.090	0.993	2.870	0.095
T16-43C2	2.945	0.093	0.978		
T16-43C3	2.867	0.103	0.989		
T24-43C1	2.437	0.123	0.984	2.420	0.121
T24-43C2	2.359	0.116	0.988		
T24-43C3	2.466	0.123	0.989		
T16-54C1	4.815	0.155	0.995	4.794	0.142
T16-54C2	4.933	0.140	0.993		
T16-54C3	4.635	0.130	0.993		
T24-54C1	4.050	0.168	0.997	3.979	0.174
T24-54C2	3.975	0.180	0.997		
T24-54C3	3.912	0.174	0.995		

(1) Load on one span
(2) Average deflection of both spans.

5.5 Ultimate Capacity

The ultimate capacity and corresponding vertical deflection for all top plate test specimens are listed in Table 5.3. Figure 5-5 shows the load-displacement plots for all test specimens at the same scale for comparison. Standard deviation of ultimate capacity for all specimen groups was also calculated. As expected, the 54-mil specimens support greater load

than the corresponding 43-mil specimens. In addition, the 16" span specimens support greater load than the 24" span as expected. Group T16-43 had the lowest standard deviation of only 4 pounds. Group T16-54 had the highest standard deviation compared to all other groups of 57 pounds. In general, standard deviations are within two percent of the average ultimate capacity for all groups, indicating consistent strength results for specimens in each group. The vertical deflection at ultimate capacity varies from about 1/4" to 3/8", being slightly higher for the shorter spans and thicker gauge material.

Table 5.3: Ultimate Capacity and Corresponding Deflection

Specimen	Ultimate Capacity (kip) (1)	Deflection (in) (2)	Average Ultimate Capacity (kip)	Average Deflection (in)	Standard Deviation (kip)
T16-43C1	3.839	0.344	3.839	0.356	0.004
T16-43C2	3.834	0.358			
T16-43C3	3.844	0.367			
T24-43C1	2.935	0.265	3.005	0.256	0.051
T24-43C2	3.053	0.249			
T24-43C3	3.028	0.255			
T16-54C1	6.384	0.439	6.304	0.399	0.057
T16-54C2	6.276	0.457			
T16-54C3	6.252	0.303			
T24-54C1	5.094	0.336	5.040	0.352	0.042
T24-54C2	5.036	0.362			
T24-54C3	4.992	0.358			

(1) Load on one span.
(2) Average deflection of both spans.

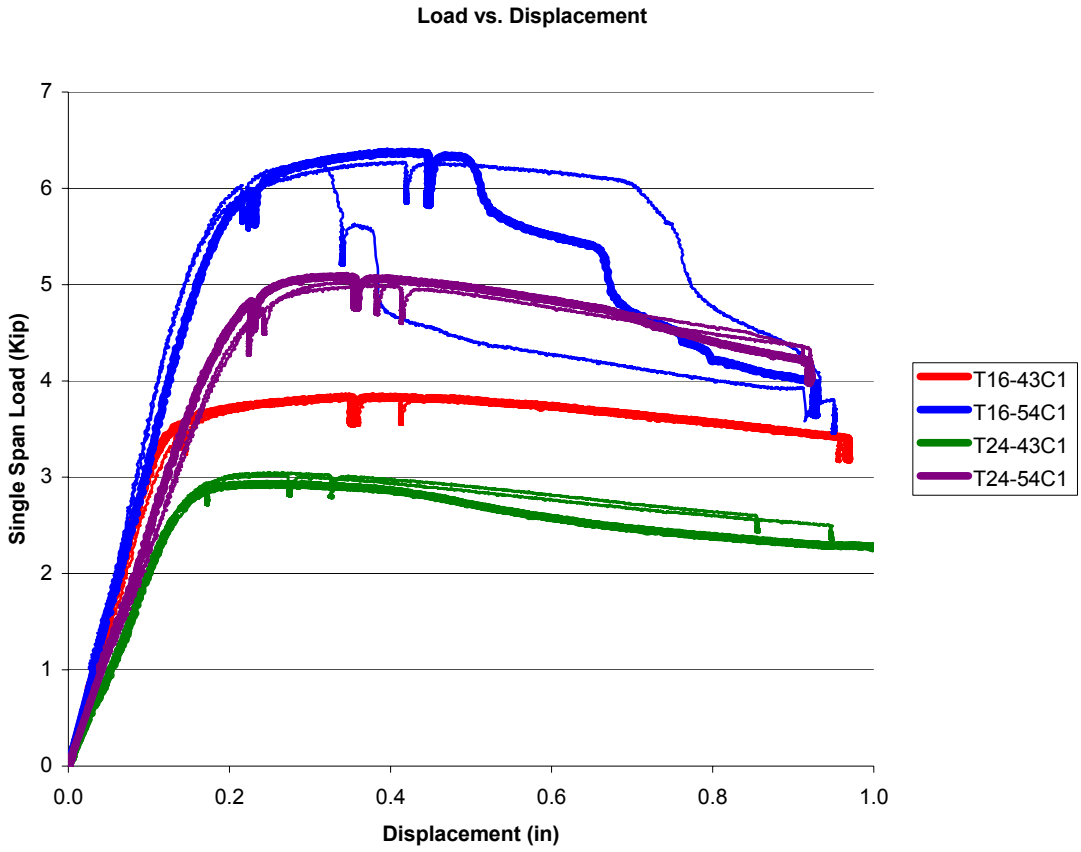

Figure 5-5: Load Displacement Curve for All Specimen

6 Analytical Study

6.1 Overview

In addition to the experimental testing, a computer analysis was performed for each specimen using LGBeamer (Devco). Due to the limitation of LGBeamer in analyzing member bending about the weak axis (y-y), the composite section was separated into individual stud and track sections for analytical purposes. Therefore, two models were generated for each specimen. The computer model was used to provide the value of the load allowed by the current building code. The material strengths used by LGBeamer are the AISI code specified 33 ksi for 43-mil material and 50 ksi for 54-mil material. These analytical results are compared with the experimental test results in Chapter 7.

6.2 Computer Modeling

6.2.1 LGBeamer

LGBeamer is a computer-modeling program made by Devco Software Inc. to specifically analyze cold-formed steel members. LGBeamer calculations are based on the American Iron and Steel Institute (AISI) "Specification for the Design of Cold-Formed Structural Members". The 1996 edition, 1996 edition with 1999 supplement, or the 2001 North American Specification, can be selected for use in the analysis. In this analytical study, the 1996 edition with 1999 supplement was selected (AISI, 1999).

This program is capable of modeling single or multi-span members with cantilevers, using different cold-formed steel sections, such as stud, joist, track and z-shaped sections. Members can be modeled under concentrated and uniformly distributed loads. Axial compressive loads can also be added to the member. The selected member can be modeled as a single, box, back to back, or built-up section. In the case of weak-axis bending, the program can only model the member as a "single" section.

Based on the AISI specification (AISI 1999), LGBeamer will also take into account the strength increase in the member by cold forming of the steel. The user can choose to include or ignore the elevated strength in the analysis. In this analytical study, the elevated strength was included per AISI specification.

Strong-axis bending can be modeled in any braced length. However, for weak-axis bending, the current building code does not give special provision. LGBeamer will analyze the member as if it were fully braced.

Punch-out members bending about their weak axis, with the web in compression, are treated in the same fashion as used for axially loaded members. The punch-outs will always reduce the strength of the member. Strength and load modifiers can also be input to include the effect of earthquake and wind load.

6.2.2 Modeling

LGBeamer has limited capability in the analysis of members bending about the weak axis. Each member in the composite section had to be analyzed individually. In the modeling procedure, the assumption is made that the twelve screws used to assemble the top track do not provide adequate strength to force the three members to act as a full composite section. Therefore, the three members are free to react individually.

A stud and a track model were generated for every specimen. Using the principle of superposition, the analysis results were added together to give the estimated capacity of the composite section even though the deflection may not have been the same. The composite section contains two tracks and a stud section. Therefore, the allowable capacity was calculated by summing the capacity of two tracks and one stud section.

The code selected for the analysis here is the AISI 1996 edition with 1999 supplement. All members of the composite top plate are bending about their weak axis. Built-in section properties were used in the analysis.

Span lengths and point load locations were input according to the actual test set-up. Load was then incrementally added until the output showed inadequate strength. Figure 6-1 shows a typical LGBeamer input screen for one of the tests specimens, while Figure 6-2 shows a typical output.

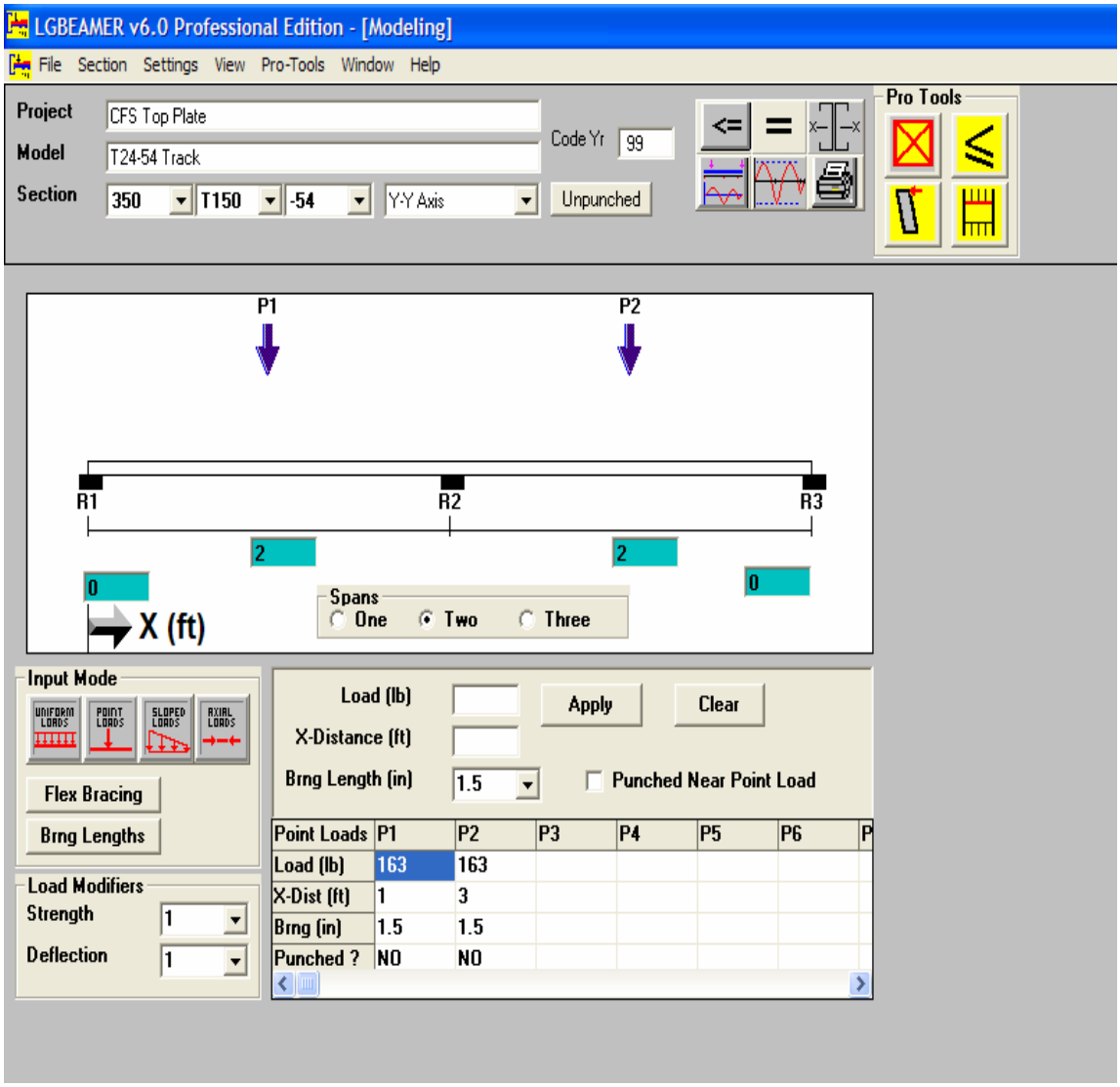

Figure 6-1: Typical Input Screen in LGBeamer

1996 AISI Specification w/1999 Supplement

Project: CFS Top Plate
Model: T16-43Stud

Date: 11/6/2005

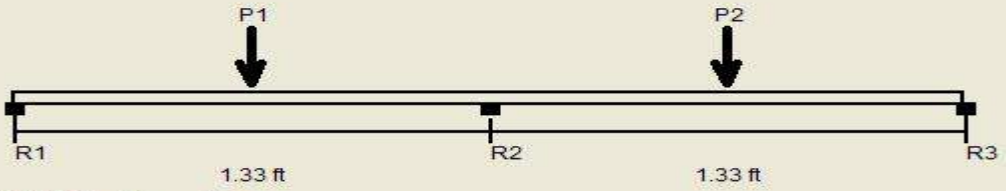

Point Loads	P1	P2
Load(lb)	545	545
X-Dist.(ft)	0.67	2.00

Section : 350S162-43 Single C Stud (Y-Y Axis) **Fy =** 33.0 ksi
Mayo = 173.0 Ft-Lb **Moment of Inertia, I =** 0.102 in^4 **Va =** 1657.8 lb

Loads have not been modified for strength checks
Loads have not been modified for deflection calculations

Flexural and Deflection Check

Span	Mmax Ft-Lb	Mmax/ Maxo	Mpos Ft-Lb	Bracing (in)	Ma(Brc) Ft-Lb	Mpos/ Ma(Brc)	Deflection (in)	Deflection Ratio
Left Span	136.2	0.787	113.5	Full	173.0	0.656	0.007	L/2306
Right Span	136.2	0.787	113.6	Full	173.0	0.656	0.007	L/2305

Combined Bending and Web Crippling

Reaction or Pt Load	Load P(lb)	Brng (in)	Pa (lb)	Mmax (Ft-Lb)	Intr. Value	Stiffen Req'd ?
R1	170.2	1.00	511.2	0.0	0.40	No
R2	749.2	1.00	1263.3	136.2	1.50	No
R3	170.5	1.00	511.2	0.0	0.40	No
P1	545.0	1.50	1348.1	113.5	1.14	No
P2	545.0	1.50	1348.1	134.7	1.26	No

Combined Bending and Shear

Reaction or Pt Load	Vmax (lb)	Mmax (Ft-Lb)	Va Factor	V/Va	M/Ma	Intr. Unstiffen	Intr. Stiffen
R1	170.2	0.0	1.00	0.10	0.00	0.01	NA
R2	374.8	136.2	1.00	0.23	0.79	0.67	NA
R3	170.5	0.0	1.00	0.10	0.00	0.01	NA
P1	374.8	113.5	1.00	0.23	0.66	0.48	NA
P2	374.5	113.4	1.00	0.23	0.66	0.48	NA

Figure 6-2: Typical Output Screen in LGBeamer

6.2.3 Results

Table 6.1 and Table 6.2 summarize the results of this analytical study. Table 6.1 lists the individual model designation, configuration and allowable load per span. Table 6.2 lists the final capacity of the composite section. Detailed outputs for each LGBeamer model are provided in Appendix A.

Table 6.1: Individual Member Analysis Results

Model	Span Length (Inch)	Section Thickness (mil)	Section Type	Single Span Load Capacity (lbs)
T16-43Stud	16	43	Stud	545
T16-43 Track	16	43	Track	120
T24-43 Stud	24	43	Stud	431
T24-43 Track	24	43	Track	80
T16-54 Stud	16	54	Stud	1065
T16-54 Track	16	54	Track	245
T24-54 Stud	24	54	Stud	830
T24-54 Track	24	54	Track	163

Table 6.2: Combined Capacity for Each Composite Top Plate Section

Composite Section	Load Capacity: 1 Stud + 2 Tracks (lbs)
T16-43	785
T24-43	591
T16-54	1555
T24-54	1156

7 Discussion

7.1 Overview

This chapter presents comparisons of the different top plate test configurations and comparison of the experimental and analytical results. Three main topics discussed are the comparison between specimens with different span length and material thickness, and comparison of experimental results versus computer analysis.

7.2 Comparison of 16" and 24" Span Specimens

As expected, all specimens with shorter spans have a higher load carrying capacity than equivalent specimens with longer spans. There is also a slight decrease in deflection at the proportional limit for shorter span specimens. Between the 16" and 24" group at proportional limit, an average of 20% decrease in deflection was recorded. At the same point, load carrying capacities had an increase of about 18% to 20%. This is to be expected as the specimens are still responding elastically up to the proportional limit. An average of 26% increase in load was noted at ultimate capacity for the shorter spans. The deflections at ultimate load are very similar between the different span specimens, with an average of 0.34" (approx. 3/8").

7.3 Comparison of 43-mil and 54-mil

As expected, all thicker gauge specimens had increased capacity compared to their thinner gauge counterparts. For an increase of only 26% (11-mil) in thickness, the flexural capacity at both proportional limit and ultimate capacity increased by 64% to 67%. Since applied loads were larger in the 54-mil specimens, local web buckling near the center support became more critical. By visual inspection, the deformation of the track flanges was greater than those in the 43-mil specimens. In group T16-54, the local buckling of the track flanges may have initiated the buckling failure of the center support stud.

7.4 Comparison of Analytical Allowable Load and Proportional Limit

Table 7.1 summarizes the results from the experimental tests and computer analysis. In general, the allowed load from the AISI code analysis is much smaller than the capacity of the member. In comparison to the proportional limit, the code allowable loads are about 30% of the member capacity. In the computer analysis, the load was added until either the member reach maximum stress or a stiffener is required to prevent buckling. During testing, no signs of deformation, local buckling or bearing failure were observed until the member exceeded about 60% of the proportional limit. As the stiffness of the top plate increases, the code allows a higher percentage of the capacity to be used in comparison with both proportional limit and ultimate capacity.

Table 7.1: Analytical Allowable Load and Proportional Limit

Specimen	Code Allowable Load (lbs)	Proportional limit (lbs)	Percentage of Proportional limit (%)	Ultimate Load (lbs)	Percentage of Ultimate Load (%)
T16-43	785	2870	27.4	3839	20.5
T24-43	591	2420	24.4	3005	19.7
T16-54	1555	4794	32.4	6304	24.7
T24-54	1156	3979	29.1	5040	22.9

8 Conclusions and Recommendations

8.1 Conclusions

Based on the results of this study the following conclusions were made:

- Cold-formed steel (CFS) load-bearing walls with composite top plates consisting of a stud and two tracks in the configuration tested in this study are capable of supporting non-concentric loads from joists, studs and rafters bearing on the wall.
- Based on an AISI code allowable load analysis performed using the computer program LGBeamer, the average allowable load for all specimens is approximately 30% of the experimentally determined proportional limit.
- The LGBeamer average allowable load for all specimens is approximately 22% of the experimentally determined ultimate capacity (Factor of Safety of 4.5).
- Specimens with 16" spans supported 18% to 20% greater load at the proportional limit than identical specimens with 24" spans. There was a corresponding 20% decrease in deflection at the proportional limit for the shorter span specimens.
- Top plate specimens with 54-mil material thickness showed a strength gain of about 65% over 43-mil material at both proportional limit and ultimate capacity.
- Vertical deflections at ultimate load were similar for all specimens regardless of span length or material thickness, for the parameters tested in this study. The average deflection for all specimens at ultimate load was 0.34" (approx 3/8").

8.2 Recommendations

Based on the results of this study, composite top plate sections consisting of one stud and two tracks of the same material thickness can be used to distribute vertical loads in non-concentric CFS framing. The minimum material thickness to be used for the top plate sections is 43-mil (18 gauge), and the sections must be constructed using #10 screws as described in this report. The stud sections used in the top plate are assumed to contain punch-outs. If studs without punch-outs are used, the allowable load can be increased by 10%, however field inspection is recommended to ensure un-punched studs are used for the top plate sections.

Assuming a safety factor of 3.0 against failure, and 2.5 against non-linear response, Table 8.1 provides allowable loads for the top plate configurations tested in this study. At these allowable loads, the anticipated deflections are all less than 0.07 inches (about 1/16").

Table 8.1: Design Allowable Loads for Midspan Point Loading

Stud Spacing (inch)	Top Track Thickness (mil)	Top Track Gauge	Allowable Load (Pounds)	Estimated Deflection (inch)
24	43	18	950	0.048
16	43	18	1150	0.038
24	54	16	1600	0.070
16	54	16	1900	0.056

References

AISI (1999) "Specification for the Design of Cold-Formed Steel Structural Members" American Iron and Steel Institute, Washington D.C.

Dawe, J.L. (2005) "Experimental Evaluation of The Strength and Behavior of 16- and 18-Gauge Cold Formed Steel Top Track System –92mm and 152mm, 16"- and 24"-Spans". University of New Brunswick Structural Engineering Laboratory. NB. Canada. September 2005.

Devco Software Inc. "LGBEAMER V6.0 Professional Edition" Corvallis, OR.

NAHB (2002) "Cold-Formed Steel Top Load Bearing Tracks". National Association of Home Builders. NAHB Research Center, Upper Marlboro, MD. August 2002.

9 Appendix A

1996 AISI Specification w/1999 Supplement

Project: CFS Top Plate
Model: T16-43Stud

Date: 11/6/2005

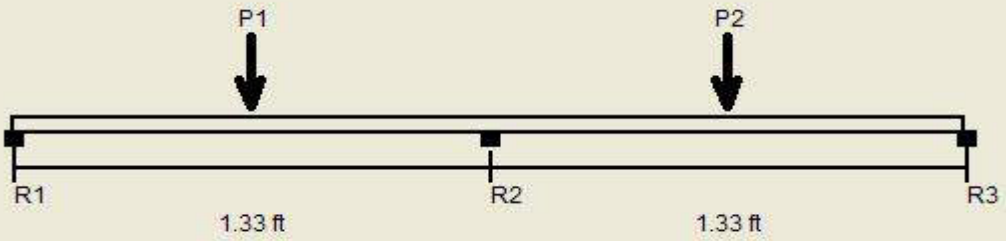

Point Loads	P1	P2
Load(lb)	545	545
X-Dist.(ft)	0.67	2.00

Section : 350S162-43 Single C Stud (Y-Y Axis) **Fy =** 33.0 ksi
Mayo = 173.0 Ft-Lb **Moment of Inertia, I =** 0.102 in^4 **Va =** 1657.8 lb

Loads have not been modified for strength checks
Loads have not been modified for deflection calculations

Flexural and Deflection Check

Span	Mmax Ft-Lb	Mmax/ Maxo	Mpos Ft-Lb	Bracing (in)	Ma(Brc) Ft-Lb	Mpos/ Ma(Brc)	Deflection (in)	Deflection Ratio
Left Span	136.2	0.787	113.5	Full	173.0	0.656	0.007	L/2306
Right Span	136.2	0.787	113.6	Full	173.0	0.656	0.007	L/2305

Combined Bending and Web Crippling

Reaction or Pt Load	Load P(lb)	Brng (in)	Pa (lb)	Mmax (Ft-Lb)	Intr. Value	Stiffen Req'd ?
R1	170.2	1.00	511.2	0.0	0.40	No
R2	749.2	1.00	1263.3	136.2	1.50	No
R3	170.5	1.00	511.2	0.0	0.40	No
P1	545.0	1.50	1348.1	113.5	1.14	No
P2	545.0	1.50	1348.1	134.7	1.26	No

Combined Bending and Shear

Reaction or Pt Load	Vmax (lb)	Mmax (Ft-Lb)	Va Factor	V/Va	M/Ma	Intr. Unstiffen	Intr. Stiffen
R1	170.2	0.0	1.00	0.10	0.00	0.01	NA
R2	374.8	136.2	1.00	0.23	0.79	0.67	NA
R3	170.5	0.0	1.00	0.10	0.00	0.01	NA
P1	374.8	113.5	1.00	0.23	0.66	0.48	NA
P2	374.5	113.4	1.00	0.23	0.66	0.48	NA

Figure 9-1: T16-43 Stud Analysis Results

1996 AISI Specification w/1999 Supplement

Project: CFS Top Plate
Model: T16-43 Track

Date: 11/6/2005

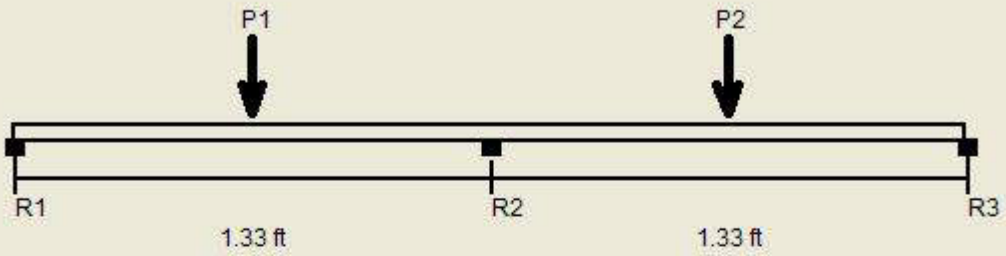

Point Loads	P1	P2
Load(lb)	120	120
X-Dist.(ft)	0.67	2.00

Section : 350T150-43 Single (Y-Y Axis) **Fy =** 33.0 ksi
Mayo = 30.2 Ft-Lb **Moment of Inertia, I =** 0.021 in^4 **Va =** 1647.5 lb

Loads have not been modified for strength checks
Loads have not been modified for deflection calculations

Flexural and Deflection Check

Span	Mmax Ft-Lb	Mmax/ Maxo	Mpos Ft-Lb	Bracing (in)	Ma(Brc) Ft-Lb	Mpos/ Ma(Brc)	Deflection (in)	Deflection Ratio
Left Span	30.0	0.992	25.0	Full	30.2	0.825	0.007	L/2206
Right Span	30.0	0.992	25.0	Full	30.2	0.827	0.007	L/2205

Combined Bending and Web Crippling

Reaction or Pt Load	Load P(lb)	Brng (in)	Pa (lb)	Mmax (Ft-Lb)	Intr. Value	Stiffen Req'd ?
R1	37.5	1.00	511.3	0.0	0.09	No
R2	165.0	1.00	1263.6	30.0	1.15	No
R3	37.5	1.00	511.3	0.0	0.09	No
P1	120.0	1.50	1348.5	25.0	0.93	No
P2	120.0	1.50	1348.5	25.0	0.93	No

Combined Bending and Shear

Reaction or Pt Load	Vmax (lb)	Mmax (Ft-Lb)	Va Factor	V/Va	M/Ma	Intr. Unstiffen	Intr. Stiffen
R1	37.5	0.0	1.00	0.02	0.00	0.00	NA
R2	82.5	30.0	1.00	0.05	0.99	0.99	NA
R3	37.5	0.0	1.00	0.02	0.00	0.00	NA
P1	82.5	25.0	1.00	0.05	0.83	0.68	NA
P2	82.5	25.0	1.00	0.05	0.83	0.68	NA

Figure 9-2: T16-43 Track Analysis Results

1996 AISI Specification w/1999 Supplement

Project: CFS Top Plate
Model: T16-54 Stud

Date: 11/6/2005

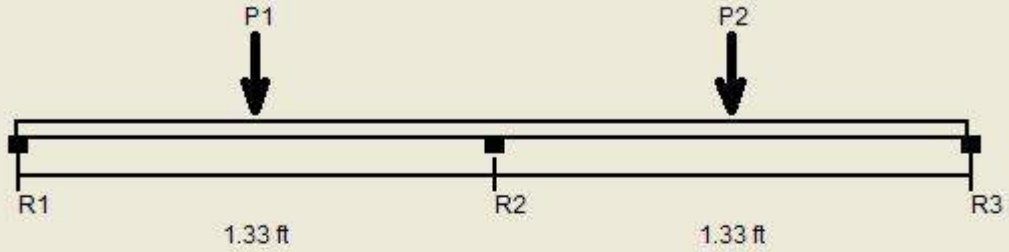

Point Loads	P1	P2
Load(lb)	1065	1065
X-Dist.(ft)	0.67	2.00

Section : 350S162-54 Single C Stud (Y-Y Axis) **Fy =** 50.0 ksi
Mayo = 319.4 Ft-Lb **Moment of Inertia, I =** 0.124 in^4 **Va =** 3038.3 lb

Loads have not been modified for strength checks
Loads have not been modified for deflection calculations

Flexural and Deflection Check

Span	Mmax Ft-Lb	Mmax/ Maxo	Mpos Ft-Lb	Bracing (in)	Ma(Brc) Ft-Lb	Mpos/ Ma(Brc)	Deflection (in)	Deflection Ratio
Left Span	266.2	0.833	221.6	Full	319.4	0.694	0.011	L/1438
Right Span	266.2	0.833	221.9	Full	319.4	0.695	0.011	L/1438

Combined Bending and Web Crippling

Reaction or Pt Load	Load P(lb)	Brng (in)	Pa (lb)	Mmax (Ft-Lb)	Intr. Value	Stiffen Req'd ?
R1	332.4	1.00	1065.4	0.0	0.37	No
R2	1464.4	1.00	2639.6	266.2	1.50	No
R3	333.2	1.00	1065.4	0.0	0.38	No
P1	1065.0	1.50	2784.8	221.6	1.15	No
P2	1065.0	1.50	2784.8	51.0	0.62	No

Combined Bending and Shear

Reaction or Pt Load	Vmax (lb)	Mmax (Ft-Lb)	Va Factor	V/Va	M/Ma	Intr. Unstiffen	Intr. Stiffen
R1	332.4	0.0	1.00	0.11	0.00	0.01	NA
R2	732.6	266.2	1.00	0.24	0.83	0.75	NA
R3	333.2	0.0	1.00	0.11	0.00	0.01	NA
P1	732.6	221.6	1.00	0.24	0.69	0.54	NA
P2	731.8	221.6	1.00	0.24	0.69	0.54	NA

Figure 9-3:T16-54 Stud Analysis Results

1996 AISI Specification w/1999 Supplement

Project: CFS Top Plate
Model: T16-54 Track

Date: 11/6/2005

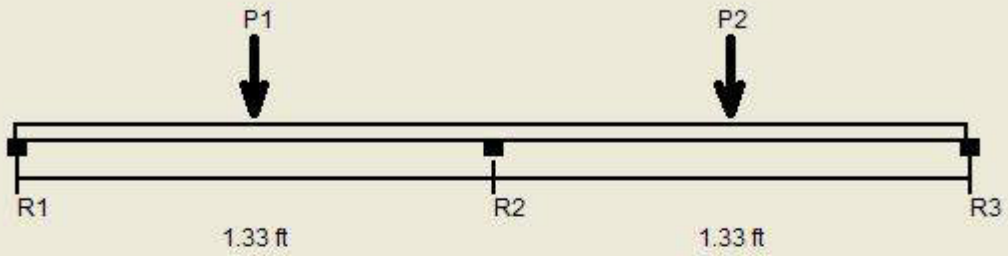

Point Loads	P1	P2
Load(lb)	245	245
X-Dist.(ft)	0.67	2.00

Section : 350T150-54 Single (Y-Y Axis) **Fy =** 50.0 ksi
Mayo = 61.5 Ft-Lb **Moment of Inertia, I =** 0.029 in^4 **Va =** 3075.6 lb

Loads have not been modified for strength checks
Loads have not been modified for deflection calculations

Flexural and Deflection Check

Span	Mmax Ft-Lb	Mmax/ Maxo	Mpos Ft-Lb	Bracing (in)	Ma(Brc) Ft-Lb	Mpos/ Ma(Brc)	Deflection (in)	Deflection Ratio
Left Span	61.2	0.996	51.0	Full	61.5	0.829	0.011	L/1471
Right Span	61.2	0.996	51.1	Full	61.5	0.831	0.011	L/1470

Combined Bending and Web Crippling

Reaction or Pt Load	Load P(lb)	Brng (in)	Pa (lb)	Mmax (Ft-Lb)	Intr. Value	Stiffen Req'd ?
R1	76.5	1.00	1065.0	0.0	0.09	No
R2	336.9	1.00	2638.5	61.2	1.15	No
R3	76.7	1.00	1065.0	0.0	0.09	No
P1	245.0	1.50	2783.7	51.0	0.93	No
P2	245.0	1.50	2783.7	51.2	0.94	No

Combined Bending and Shear

Reaction or Pt Load	Vmax (lb)	Mmax (Ft-Lb)	Va Factor	V/Va	M/Ma	Intr. Unstiffen	Intr. Stiffen
R1	76.5	0.0	1.00	0.02	0.00	0.00	NA
R2	168.5	61.2	1.00	0.05	1.00	1.00	NA
R3	76.7	0.0	1.00	0.02	0.00	0.00	NA
P1	168.5	51.0	1.00	0.05	0.83	0.69	NA
P2	168.3	51.0	1.00	0.05	0.83	0.69	NA

Figure 9-4: T16-54 Track Analysis Results

1996 AISI Specification w/1999 Supplement

Project: CFS Top Plate
Model: T24-43 Stud

Date: 11/6/2005

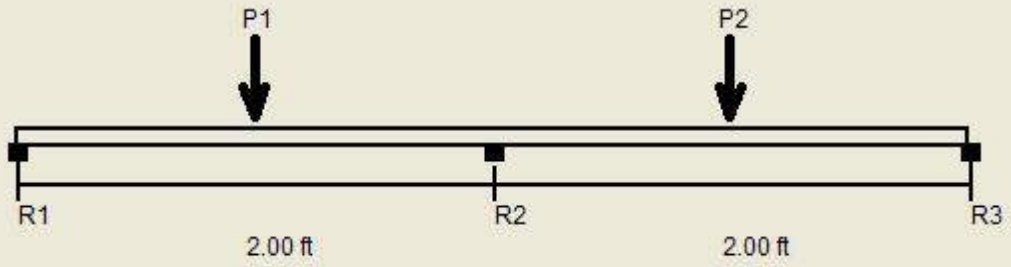

Point Loads	P1	P2
Load(lb)	431	431
X-Dist.(ft)	1.00	3.00

Section : 350S162-43 Single C Stud (Y-Y Axis) **Fy =** 33.0 ksi
Mayo = 173.0 Ft-Lb **Moment of Inertia, I =** 0.102 in^4 **Va =** 1657.8 lb

Loads have not been modified for strength checks
Loads have not been modified for deflection calculations

Flexural and Deflection Check

Span	Mmax Ft-Lb	Mmax/ Maxo	Mpos Ft-Lb	Bracing (in)	Ma(Brc) Ft-Lb	Mpos/ Ma(Brc)	Deflection (in)	Deflection Ratio
Left Span	161.6	0.934	134.7	Full	173.0	0.778	0.019	L/1295
Right Span	161.6	0.934	134.7	Full	173.0	0.778	0.019	L/1295

Combined Bending and Web Crippling

Reaction or Pt Load	Load P(lb)	Brng (in)	Pa (lb)	Mmax (Ft-Lb)	Intr. Value	Stiffen Req'd ?
R1	134.7	1.00	511.2	0.0	0.32	No
R2	592.6	1.00	1263.3	161.6	1.50	No
R3	134.7	1.00	511.2	0.0	0.32	No
P1	431.0	1.50	1348.1	134.7	1.16	No
P2	431.0	1.50	1348.1	25.0	0.53	No

Combined Bending and Shear

Reaction or Pt Load	Vmax (lb)	Mmax (Ft-Lb)	Va Factor	V/Va	M/Ma	Intr. Unstiffen	Intr. Stiffen
R1	134.7	0.0	1.00	0.08	0.00	0.01	NA
R2	296.3	161.6	1.00	0.18	0.93	0.90	NA
R3	134.7	0.0	1.00	0.08	0.00	0.01	NA
P1	296.3	134.7	1.00	0.18	0.78	0.64	NA
P2	296.3	134.7	1.00	0.18	0.78	0.64	NA

Figure 9-5: T24-43 Stud Analysis Results

1996 AISI Specification w/1999 Supplement

Project: CFS Top Plate
Model: T24-43 Track

Date: 11/6/2005

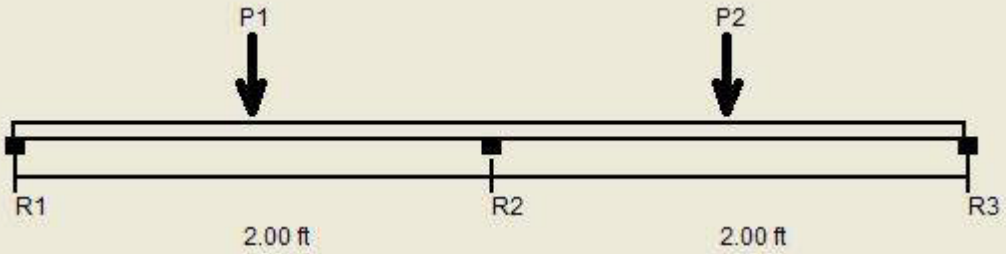

Point Loads	P1	P2
Load(lb)	80	80
X-Dist.(ft)	1.00	3.00

Section : 350T150-43 Single (Y-Y Axis) **Fy =** 33.0 ksi
Mayo = 30.2 Ft-Lb **Moment of Inertia, I =** 0.021 in^4 **Va =** 1647.5 lb

Loads have not been modified for strength checks
Loads have not been modified for deflection calculations

Flexural and Deflection Check

Span	Mmax Ft-Lb	Mmax/ Maxo	Mpos Ft-Lb	Bracing (in)	Ma(Brc) Ft-Lb	Mpos/ Ma(Brc)	Deflection (in)	Deflection Ratio
Left Span	30.0	0.992	25.0	Full	30.2	0.826	0.016	L/1470
Right Span	30.0	0.992	25.0	Full	30.2	0.826	0.016	L/1470

Combined Bending and Web Crippling

Reaction or Pt Load	Load P(lb)	Brng (in)	Pa (lb)	Mmax (Ft-Lb)	Intr. Value	Stiffen Req'd ?
R1	25.0	1.00	511.3	0.0	0.06	No
R2	110.0	1.00	1263.6	30.0	1.10	No
R3	25.0	1.00	511.3	0.0	0.06	No
P1	80.0	1.50	1348.5	25.0	0.90	No
P2	80.0	1.50	1348.5	24.7	0.89	No

Combined Bending and Shear

Reaction or Pt Load	Vmax (lb)	Mmax (Ft-Lb)	Va Factor	V/Va	M/Ma	Intr. Unstiffen	Intr. Stiffen
R1	25.0	0.0	1.00	0.02	0.00	0.00	NA
R2	55.0	30.0	1.00	0.03	0.99	0.98	NA
R3	25.0	0.0	1.00	0.02	0.00	0.00	NA
P1	55.0	25.0	1.00	0.03	0.83	0.68	NA
P2	55.0	25.0	1.00	0.03	0.83	0.68	NA

Figure 9-6: T24-43 Track Analysis Results

1996 AISI Specification w/1999 Supplement

Project: CFS Top Plate
Model: T24-54 Stud

Date: 11/6/2005

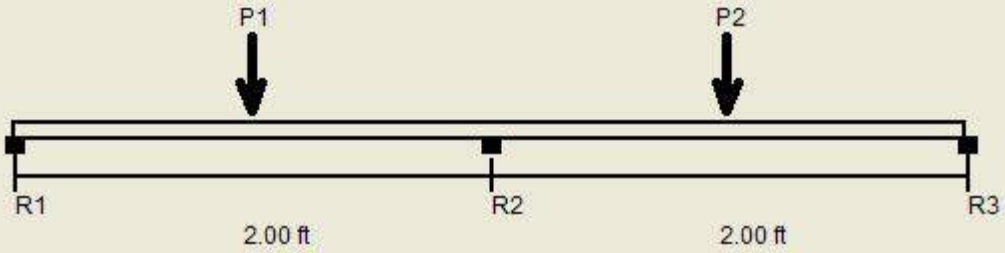

Point Loads	P1	P2
Load(lb)	830	830
X-Dist.(ft)	1.00	3.00

Section : 350S162-54 Single C Stud (Y-Y Axis) **Fy =** 50.0 ksi
Mayo = 319.4 Ft-Lb **Moment of Inertia, I =** 0.124 in^4 **Va =** 3038.3 lb

Loads have not been modified for strength checks
Loads have not been modified for deflection calculations

Flexural and Deflection Check

Span	Mmax Ft-Lb	Mmax/ Maxo	Mpos Ft-Lb	Bracing (in)	Ma(Brc) Ft-Lb	Mpos/ Ma(Brc)	Deflection (in)	Ratio
Left Span	311.2	0.974	259.4	Full	319.4	0.812	0.029	L/820
Right Span	311.2	0.974	259.4	Full	319.4	0.812	0.029	L/820

Combined Bending and Web Crippling

Reaction or Pt Load	Load P(lb)	Brng (in)	Pa (lb)	Mmax (Ft-Lb)	Intr. Value	Stiffen Req'd ?
R1	259.4	1.00	1065.4	0.0	0.29	No
R2	1141.3	1.00	2639.6	311.2	1.49	No
R3	259.4	1.00	1065.4	0.0	0.29	No
P1	830.0	1.50	2784.8	259.4	1.17	No
P2	830.0	1.50	2784.8	50.9	0.52	No

Combined Bending and Shear

Reaction or Pt Load	Vmax (lb)	Mmax (Ft-Lb)	Va Factor	V/Va	M/Ma	Intr. Unstiffen	Intr. Stiffen
R1	259.4	0.0	1.00	0.09	0.00	0.01	NA
R2	570.6	311.2	1.00	0.19	0.97	0.98	NA
R3	259.4	0.0	1.00	0.09	0.00	0.01	NA
P1	570.6	259.4	1.00	0.19	0.81	0.69	NA
P2	570.6	259.4	1.00	0.19	0.81	0.69	NA

Figure 9-7: T24-54 Stud Analysis Results

1996 AISI Specification w/1999 Supplement

Project: CFS Top Plate
Model: T24-54 Track

Date: 11/6/2005

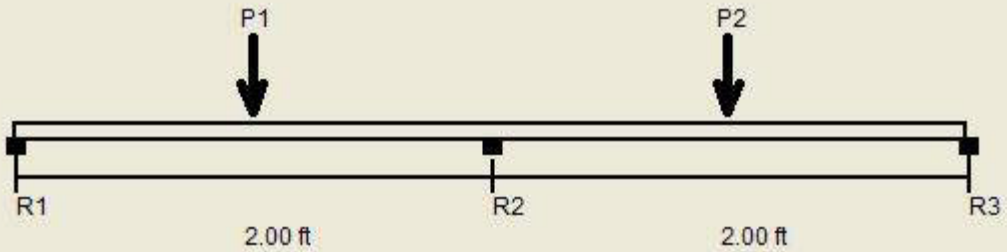

Point Loads	P1	P2
Load(lb)	163	163
X-Dist.(ft)	1.00	3.00

Section : 350T150-54 Single (Y-Y Axis) **Fy =** 50.0 ksi
Mayo = 61.5 Ft-Lb **Moment of Inertia, I =** 0.029 in^4 **Va =** 3075.6 lb

Loads have not been modified for strength checks
Loads have not been modified for deflection calculations

Flexural and Deflection Check

Span	Mmax Ft-Lb	Mmax/ Maxo	Mpos Ft-Lb	Bracing (in)	Ma(Brc) Ft-Lb	Mpos/ Ma(Brc)	Deflection (in)	Deflection Ratio
Left Span	61.1	0.994	50.9	Full	61.5	0.829	0.024	L/982
Right Span	61.1	0.994	50.9	Full	61.5	0.829	0.024	L/982

Combined Bending and Web Crippling

Reaction or Pt Load	Load P(lb)	Brng (in)	Pa (lb)	Mmax (Ft-Lb)	Intr. Value	Stiffen Req'd ?
R1	50.9	1.00	1065.0	0.0	0.06	No
R2	224.1	1.00	2638.5	61.1	1.10	No
R3	50.9	1.00	1065.0	0.0	0.06	No
P1	163.0	1.50	2783.7	50.9	0.90	No
P2	163.0	1.50	2783.7	50.9	0.90	No

Combined Bending and Shear

Reaction or Pt Load	Vmax (lb)	Mmax (Ft-Lb)	Va Factor	V/Va	M/Ma	Intr. Unstiffen	Intr. Stiffen
R1	50.9	0.0	1.00	0.02	0.00	0.00	NA
R2	112.1	61.1	1.00	0.04	0.99	0.99	NA
R3	50.9	0.0	1.00	0.02	0.00	0.00	NA
P1	112.1	50.9	1.00	0.04	0.83	0.69	NA
P2	112.1	50.9	1.00	0.04	0.83	0.69	NA

Figure 9-8: T24-54 Track Analysis Results

10 Appendix B

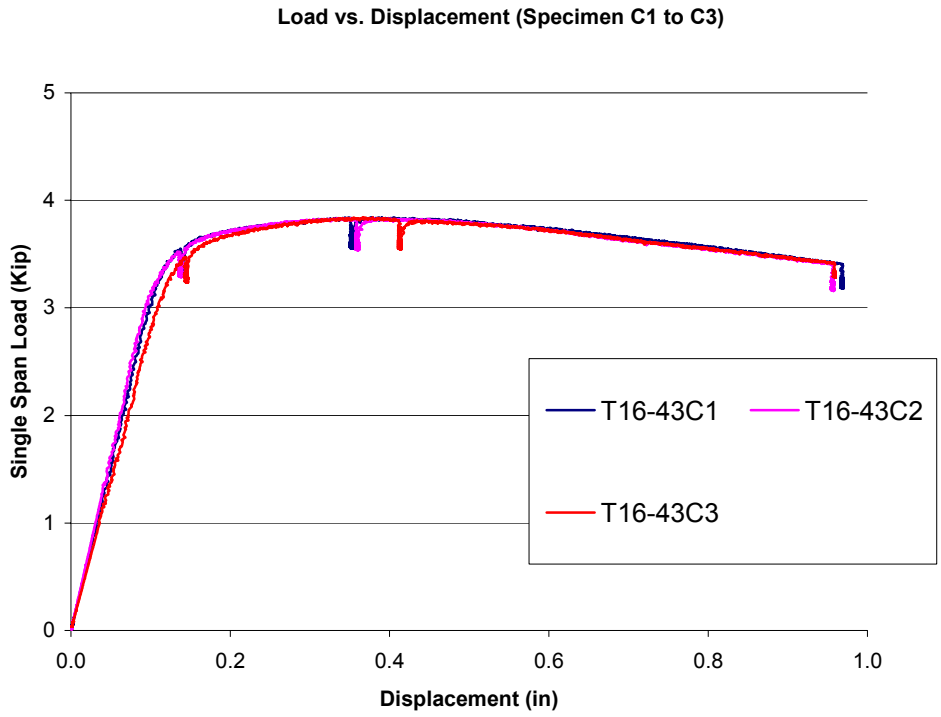

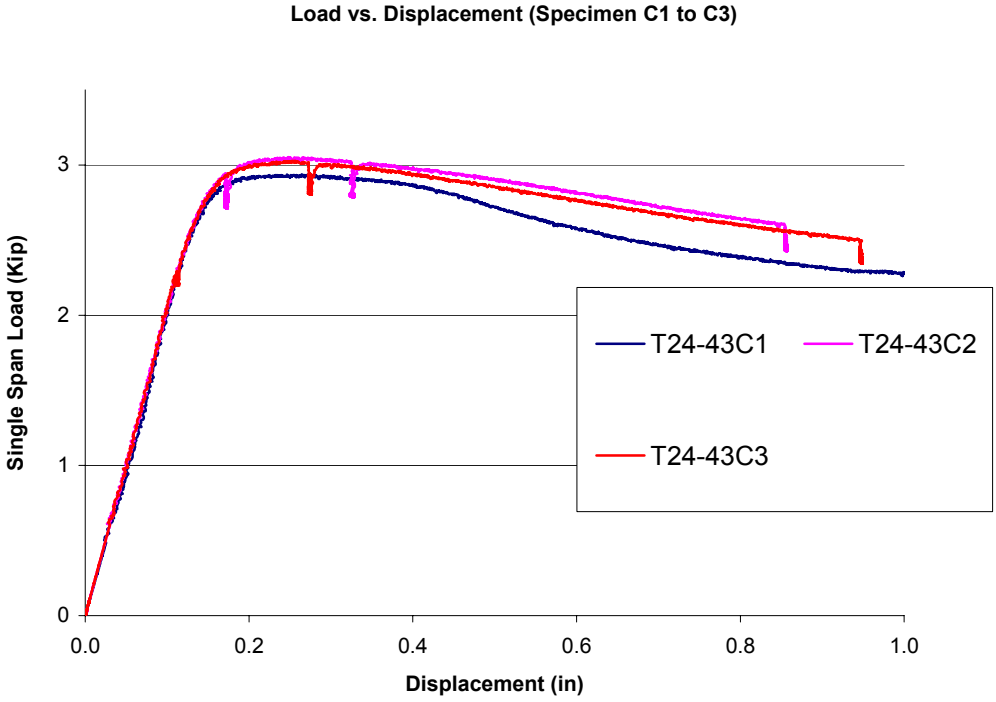

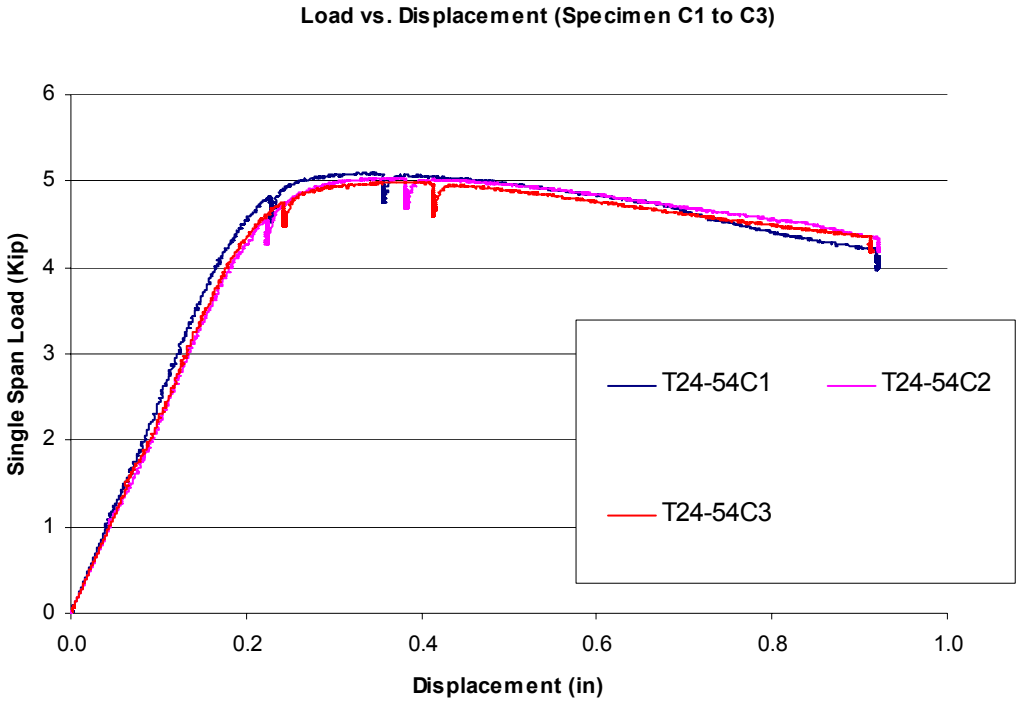
Load vs. Displacement (Specimen C1 to C3)
Single Span Load (Kip)
0
1
2
3
4
5
6
0.0
0.2
0.4
0.6
0.8
1.0
Displacement (in)
T24-54C1
T24-54C2
T24-54C3

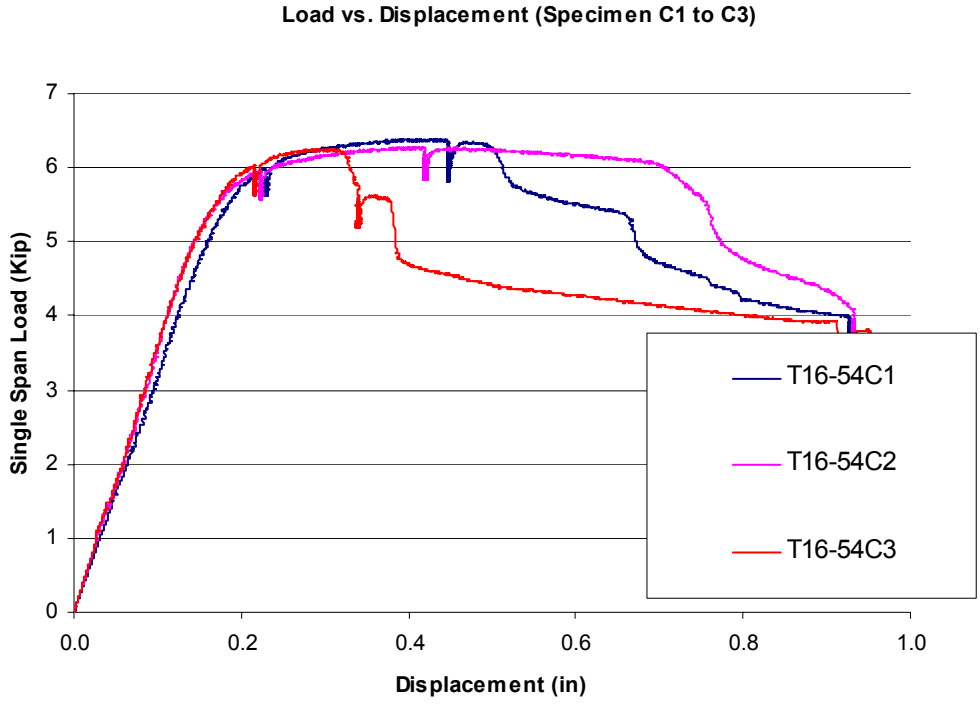
Load vs. Displacement (Specimen C1 to C3)
Single Span Load (Kip)
0
1
2
3
4
5
6
7
0.0
0.2
0.4
0.6
0.8
1.0
Displacement (in)
T16-54C1
T16-54C2
T16-54C3